Oceanic fronts control the distribution of dissolved barium in the Southern Ocean

Kimberley M. Pyle[1], Katharine R. Hendry[1]*, Robert M. Sherrell[2], Oliver Legge[3], Andrew J. Hind[3], Dorothee Bakker[3], Hugh Venables[4] and Michael P. Meredith[4]

[1] School of Earth Sciences, University of Bristol, Wills Memorial Building, Queen's Road, Bristol, BS8 1RJ, UK

[2] Department of Marine and Coastal Sciences and Department of Earth and Planetary Sciences, Rutgers University, New Jersey, USA

[3] Centre for Ocean and Atmospheric Sciences, School of Environmental Sciences, University of East Anglia, Norwich, NR4 7TJ, UK

[4] British Antarctic Survey, High Cross, Madingley Road, Cambridge, CB3 0ET, UK

*Corresponding author

Supplementary information

1. Macronutrient analyses

Dissolved inorganic nutrients (silicic acid, phosphate, and nitrate + nitrite) were analysed at the University of East Anglia using a San++ Gas Segmented Continuous Flow Analyser (Skalar, Breda, The Netherlands).

Stock solutions were prepared as mixed standards using dry analytical grade $NaNO_3$, Na_2SiF_6 and Na_2HPO_4. The quantities were weighed using a certified balance to 4 decimal places (grams scale) and were dissolved in ultrapure water (the water volume was determined gravimetrically). A working solution was prepared from the stock solution (at room temperature) using a certified pipette and saltwater (made from ultrapure water containing baked 35g/L NaCl). Dilutions of this stock into saline solution were made using the Skalar autosampler dilution function to produce standards with a range of concentrations.

The accuracy of the lab-made stock standard was confirmed using routinely analysed Certified Reference Materials (CRMs). The same nutrient stock solution used to make the saltwater standards was also used to make freshwater standards and these were used for CRM checks. The CRM used for silicate and nitrate+nitrite was Environment Canada CRM "Cranberry-05" and for phosphate the Fluka Analytical CRM "Simple nutrients". These are freshwater CRMs so were not included in the seawater sample runs as the density difference causes mixing issues.

i) Oxidised nitrogen (NO_X)

Unfiltered seawater samples for NOx (and PO_4) analysis were frozen within six hours of being sampled, and stored frozen awaiting analysis. As nitrate cannot be measured directly using a segmented flow analyser, the sample was first reduced to nitrite by buffering the solution at pH 8.2 and passing it through a copperised cadmium column. The nitrite was then determined colourimetrically, using N-(1-naphthyl)ethylenediamine dihydrochloride and sulfanilamide; the intensity of the red dye was measured by a photometer using a 540 nm filter (Bendschneider and Robinson, 1952). The detection limit for this method was approximately 0.07 µM (3x the standard deviation of repeated blank measurements).

Oxidised nitrogen (NOx) therefore refers to nitrite (NO_2) + nitrate (NO_3), although note that nitrite occurs in the water column at levels typically 70 times lower than nitrate in the photic zone and approximately 52000 times lower in the aphotic zone (Gruber, 2008). The reproducibility of NOx concentrations was ± 1.70 µM (1SD), calculated by analysing eighteen sets of duplicate samples.

ii) Phosphate (PO_4)

The sample was introduced to an acidified medium containing ammonium heptamolybdate and potassium antimony (III) oxide tartrate to form an antimony-phosphomolybdate complex. This was then reduced to a blue coloured complex using ascorbic acid, and the intensity of the colour measured spectrophotomentrically using an 810 nm wavelength filter (Murphy and Riley, 1962). The detection limit of this method was approximately 0.13 µM, calculated as for the nitrate measurement. The reproducibility of PO_4 concentrations was ± 0.18 µM (1 standard deviation calculated as the square root of the mean of the variance between duplicate), calculated by analysing eighteen sets of duplicate samples.

iii) Silicic acid ($Si(OH)_4$)

As freezing and thawing samples can lead to incomplete silicic acid recovery, separate unfiltered seawater samples also were collected and kept refrigerated at 2 to 4 °C awaiting analysis. The sample was acidified with sulfuric acid and mixed with an ammonium heptamolybdate solution. This was then reduced to a blue coloured complex using ascorbic acid, and the intensity of the colour measured spectrophotometrically using an 810nm wavelength filter. Oxalic acid was added to reduce interference from phosphate. The detection limit of this method was approximately 0.09µM, calculated as for the nitrate measurement. The reproducibility of $Si(OH)_4$ concentrations was ± 1.64 µM (1SD), calculated by analysing sixteen sets of duplicate samples.

2. Polar front locations

Temperature and salinity were used to establish the location of the ACC fronts across the Drake Passage and North Scotia Ridge transects (Fig. S1-S4). The Sub-Antarctic Front, Polar Front, and the Southern ACC Front are dynamic features that can be identified by the location of enhanced horizontal gradients in near-surface temperature, salinity, and oxygen concentration, and have traditionally been considered boundaries between distinct water masses (Graham et al., 2012; Orsi et al., 1995).

Across the Drake Passage transect, the Southern Boundary is observed between Stations 7 and 9, marked most clearly in a positive sea surface temperature (SST) gradient heading northward. The location of the Southern ACC Front is indistinct in our data, possibly falling within the less-resolved mid-section of the Drake Passage. The Polar Front is located between Stations 26 and 30, with clear surface gradients toward increased SSTs, lower salinity, and lower oxygen concentrations. The Sub-Antarctic Front is also less clearly defined, but is approximated to lie between Stations 35 and 37.

Across the North Scotia Ridge Transect the Sub-Antarctic Front is again less distinct, but can be located approximately between Stations 128 and 125 by an eastward transition to a colder, less saline, less oxygenated water column. The Polar Front is observed between Stations 101 and 100, marked by an eastward increase in surface oxygen concentrations, accompanied by lowered salinity and temperature.

Within these horizontally bounded frontal zones, the vertical distribution of conservative parameters marks the transition with depth through the cores of key water masses: Antarctic Intermediate Water (AAIW), and Upper and Lower Circumpolar Deep Waters (UCDW and LCDW). These water masses are most distinctly differentiated by their oxygen concentrations. In the Drake Passage transect, AAIW can be recognised as a relatively warm, low salinity, well-oxygenated shallow water mass north of the PFZ. This overlies the Circumpolar Deep Waters, divided into the low oxygen UCDW, warmer and more saline than the deep waters of the LCDW. At the very base of the water column in the Drake Passage, the colder, slightly fresher South Pacific Deep Water (SPDW) can be distinguished from the bulk of LCDW by increased silicic acid values (Naveira Garabato et al., 2002).

Stations 30 to 41 lie north of the Polar Front (Fig. S1), in ACC waters flowing eastwards in the PFZ and SAZ. Three of these stations reach depths below 4000 m whilst Stations 37 and 40 are shallower, reaching bottom depths of 2800 m and 1525 m respectively on the continental rise/slope. The Polar Front is marked at approximately 56 °S by a notable change in the water column; the disappearance of the temperature minimum layer, and the decreased dominance of salinity on

stratification. Sea surface temperatures increase to 6 to 7 °C, with warmer temperatures and lower salinities extending down to 1000m, where subducted AAIW (4 °C; salinity 34.2) overlies low oxygen UCDW (2 °C; salinity 34.7).

Stations 9 to 26 lie north of the Southern Boundary and south of the Polar Front (Fig. S2), in the core of the eastward flowing ACC. These four stations reach depths of between 3000 and 4000 m and show a well-stratified water column with the stratification dominantly controlled by salinity; relatively warm (2 to 3°C), low salinity (33.7 to 33.8) surface waters (0 to 50 m), a temperature minimum (-1 to 0°C) at approximately 100 m, and a core of relatively warm (2 °C) saline (34.4 to 34.7) UCDW at 250 to 1000 m mixing with colder (0 to 1°C) LCDW and Weddell Sea Deep Water (WSDW) (-0.7 < T < 0 °C) bottom waters.

South of the Southern ACC Boundary, Stations 3 to 7 were sited in Antarctic continental waters. The water mass as a whole is 1 to 1.5 ^{o}C colder, with less temperature variation than the northward stations of the ACC and PFZ. Relatively warm sea surface temperatures (SSTs) (0.5 to 0.75°C; salinity 34) overlie a more saline, low temperature layer at the base of the thermocline (approximately 500 m; 0 to -0.5 °C; salinity 34.5). Below 500 m the water column is relatively homogeneous with regards to salinity and oxygen concentrations, with potential temperatures ranging from 0.75 °C to just below 0 °C at the base.

3. Barite Saturation Index calculations

Surface barium saturation indices were estimated according to (Monnin, 1999; Thomas et al., 2011) using the following equation:

$$SI = \frac{Q}{K_{sp}} = \frac{m_{Ba(aq)} \cdot m_{SO4(aq)} \cdot \gamma^{2}_{BaSO4(aq)}}{K_{sp}}$$

Where *m* denotes the molality of the species in aqueous form, K_{sp} is the solubility product, γ is the total (or stoichiometric) mean activity coefficient of aqueous barium sulphate (for the general conditions here the following assumptions were made: log K_{sp} = –10.482, γ = 0.128 kg/mol for surface temperatures 1 ±2 °C and log K_{sp} = –10.38, γ = 0.165 kg/mol for surface temperatures 5 ±1 °C (Monnin, 1999)), and Q is the ion activity product of aqueous barium sulphate. The molarity of sulphate was calculated assuming seawater concentrations of 28.23 mM at a standard salinity of 35. The molality values for sulphate were then converted from molarity using seawater density calculated from temperature, salinity and pressure measurements from the CTD. See Figure S10.

Supplementary Figures

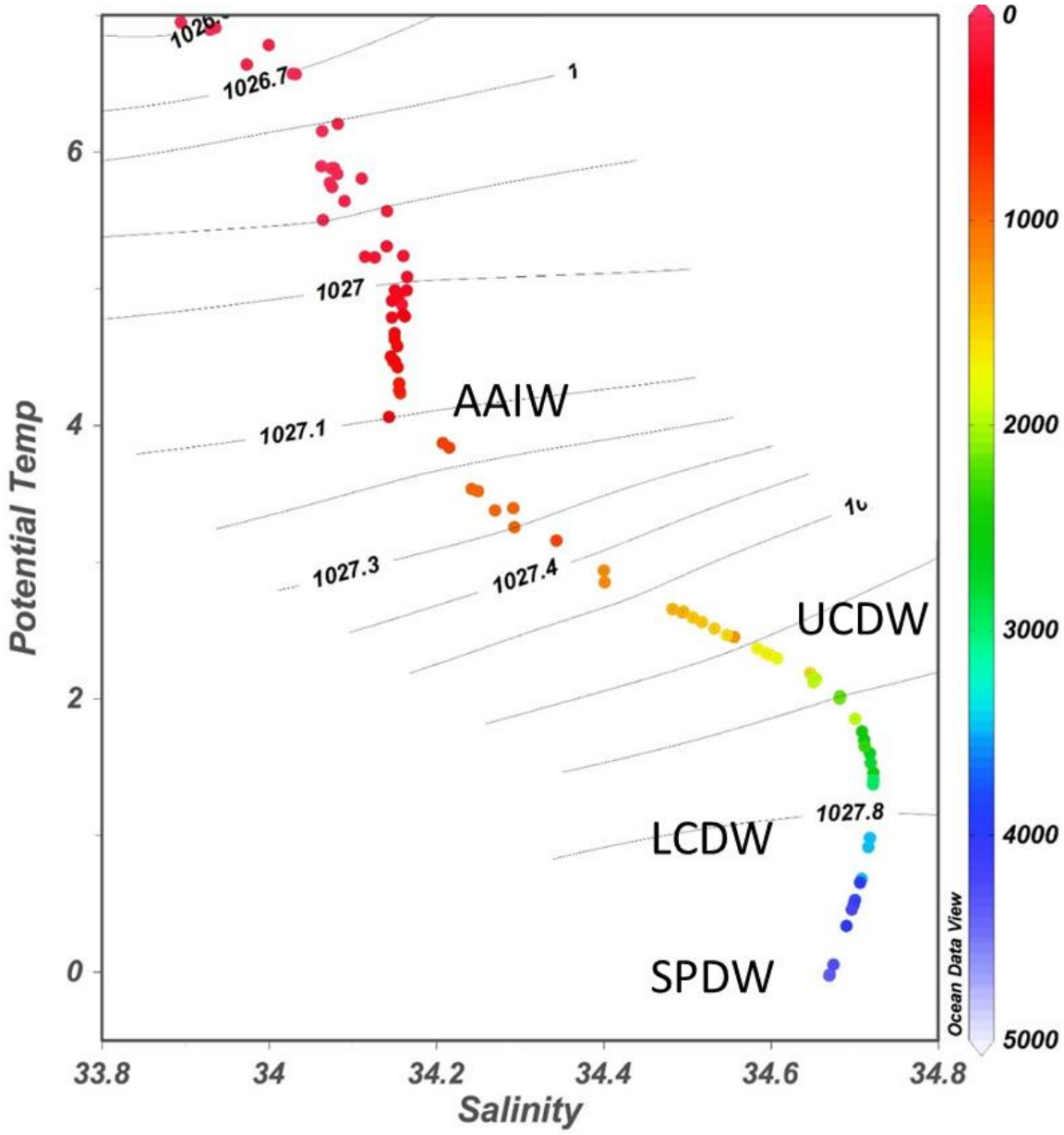

Figure S1: *Potential temperature (°C) vs. salinity for stations north of the Polar Front. Contours show density and colour scale represents depth (m) in the water column. Main water masses labelled: Antarctic Intermediate Water (AAIW), Upper and Lower Circumpolar Deep Waters (UCDW and LCDW), South Pacific Deep Water (SPDW). All T-S plots made using Ocean Data View version 4.*

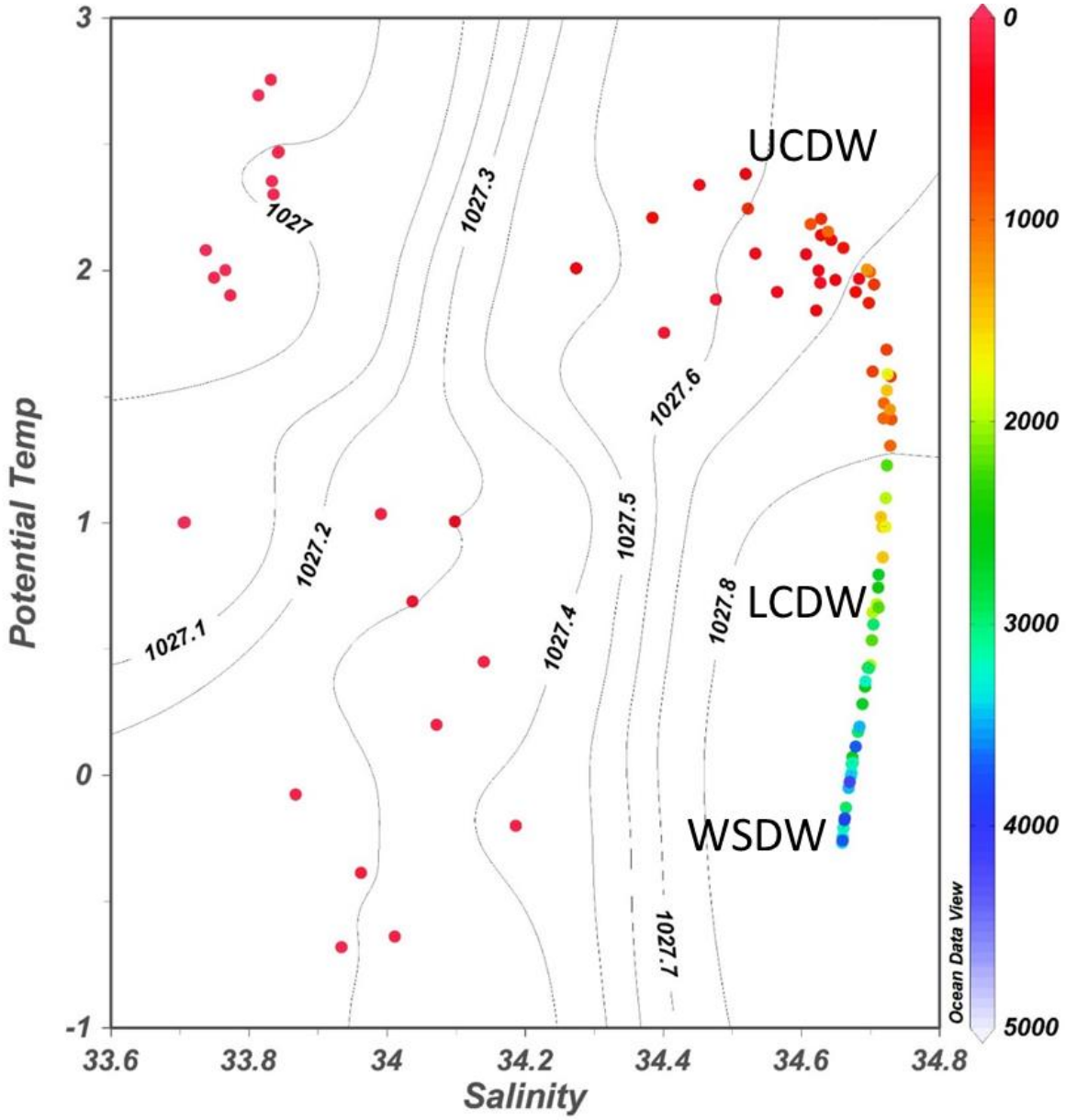

Figure S2: *Potential temperature (°C) vs. salinity for stations south of the Polar Front and north of the Southern Boundary. Contours show density and colour scale represents depth (m) in the water column. Antarctic Intermediate Water (AAIW), Upper and Lower Circumpolar Deep Waters (UCDW and LCDW), Weddell Sea Deep Water (WSDW) end-members labelled.*

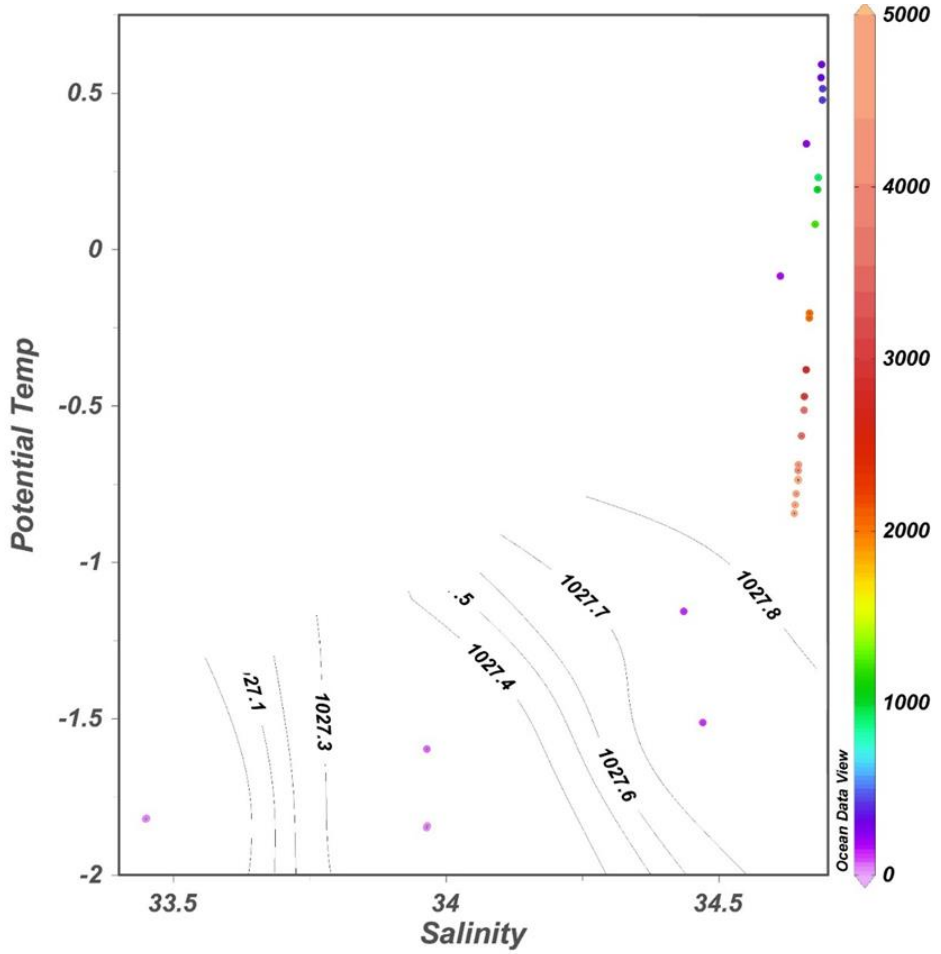

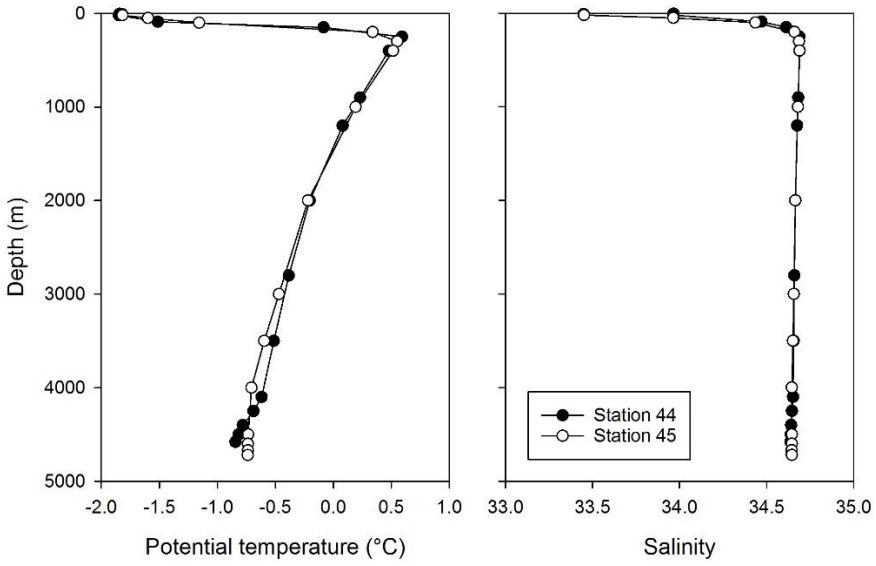

Figure S3: *Potential temperature (°C) vs. salinity plot for stations in the Weddell Sea. Contours show density and colour scale represents depth (m) in the water column. Lower plot shows T and S profiles for the same stations.*

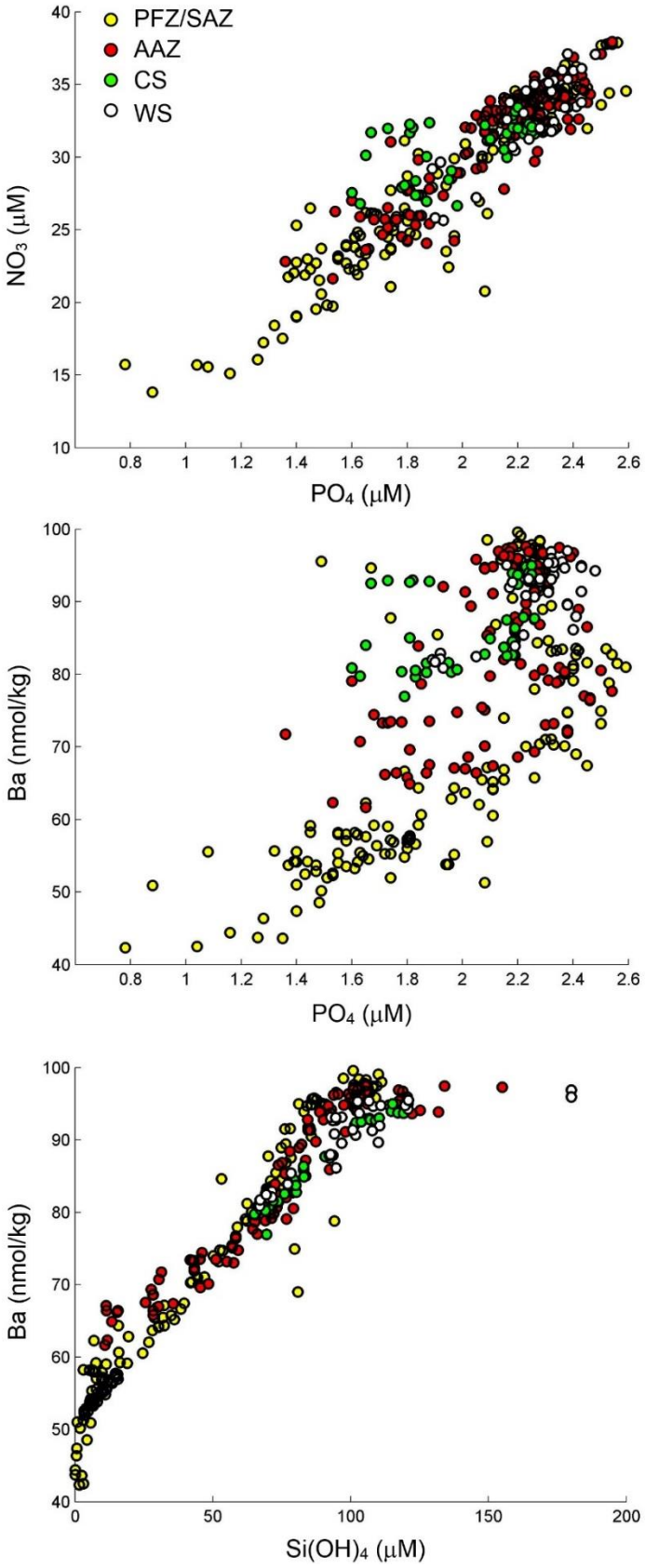

Figure S4: *Cross-plots of macronutrients from the study region. Stations north of the Polar Front (Subantarctic Zone SAZ and Polar Front Zone PFZ; JR299 Stations 30-40 from the Drake Passage Section and Stations 101-132 from the North Scotia Ridge Section) marked with yellow circles, stations south of the Polar Front marked with red circles (Antarctic Zone AAZ; Stations 9-26 from the Drake Passage Section and Stations 95-100 from the North Scotia Ridge Section). Stations south of the Southern Boundary are marked by green circles (continental shelf waters adjacent to the Peninsula CS; Stations 2-7) and white circles (Weddell Sea WS; Stations 44-45).*

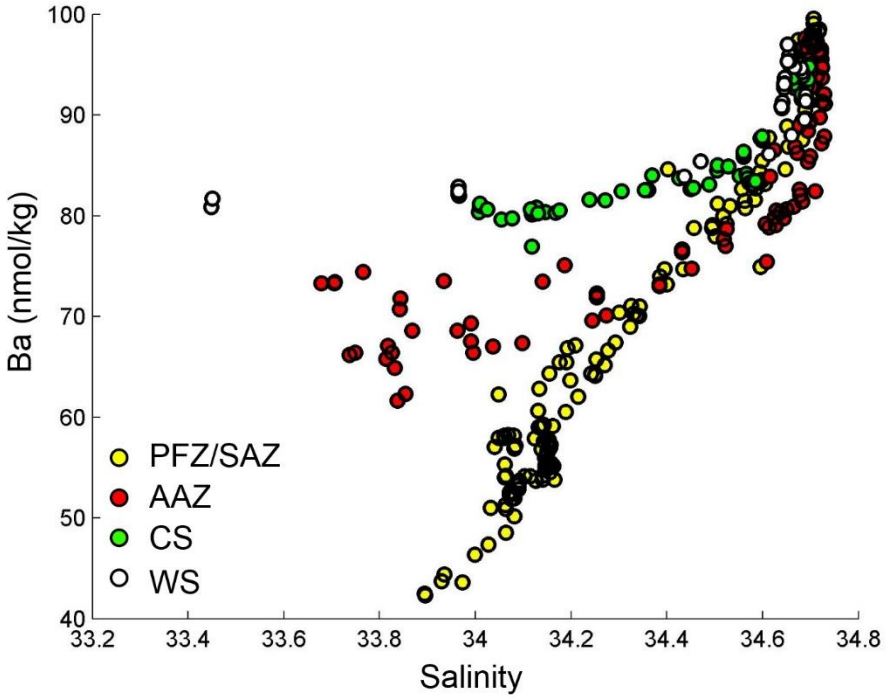

Figure S5: *Cross-plot of dissolved barium Ba_d (nmol/kg) and salinity for the study region. Note the linear relationship between Bad and salinity for waters north of the Polar Front. Symbols as per Fig. S4.*

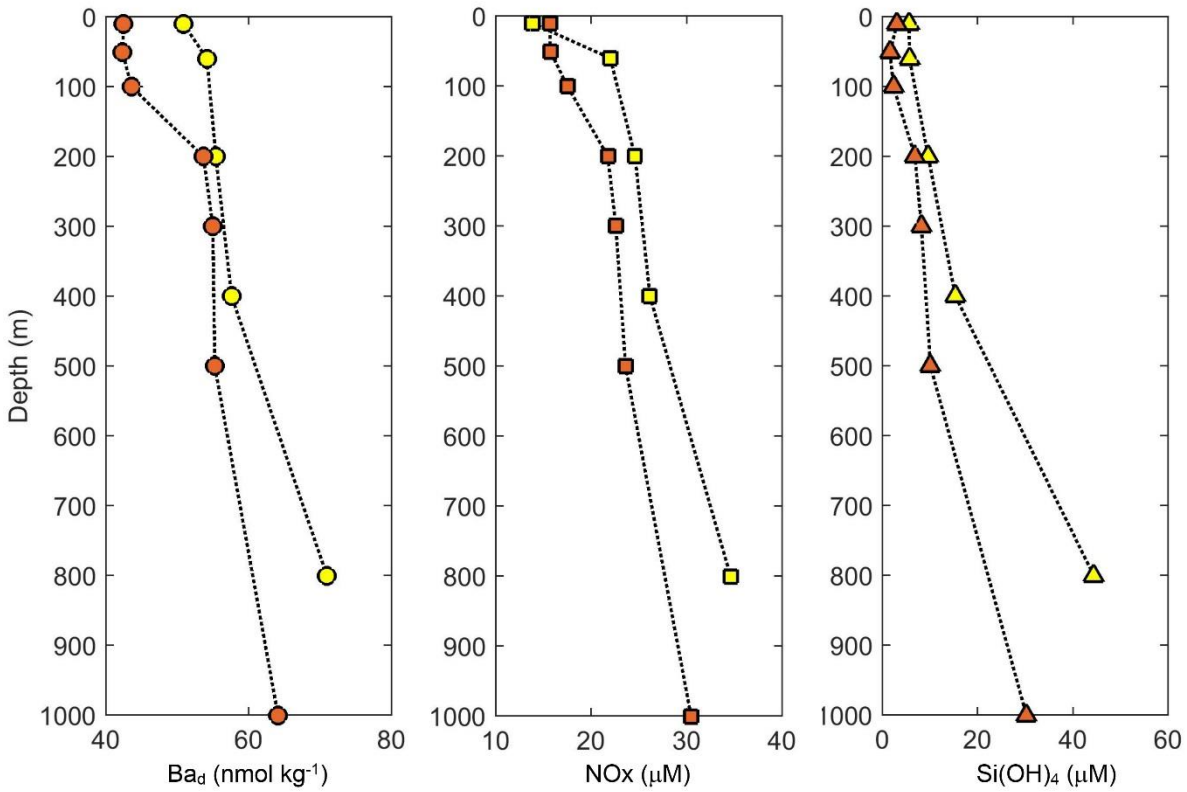

Figure S6: *Depth profiles (top 1000m) from Stations 30 (yellow) and 33 (orange) north of the Polar Front showing depth behaviour of barium (circles), nitrate (squares) and silicic acid (triangles).*

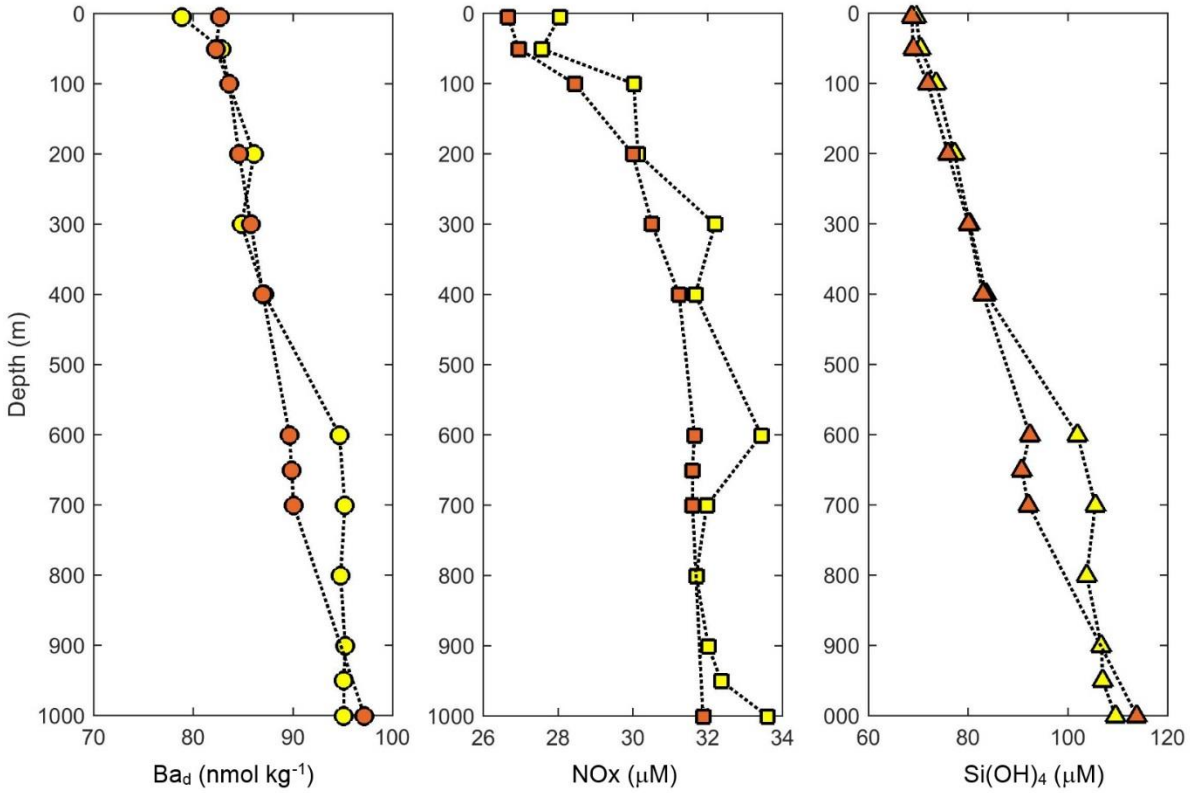

Figure S7: *Depth profiles (top 1000m) from Stations 5 (yellow) and 7 (orange) from coastal Antarctica showing depth behaviour of barium (circles), nitrate (squares) and silicic acid (triangles).*

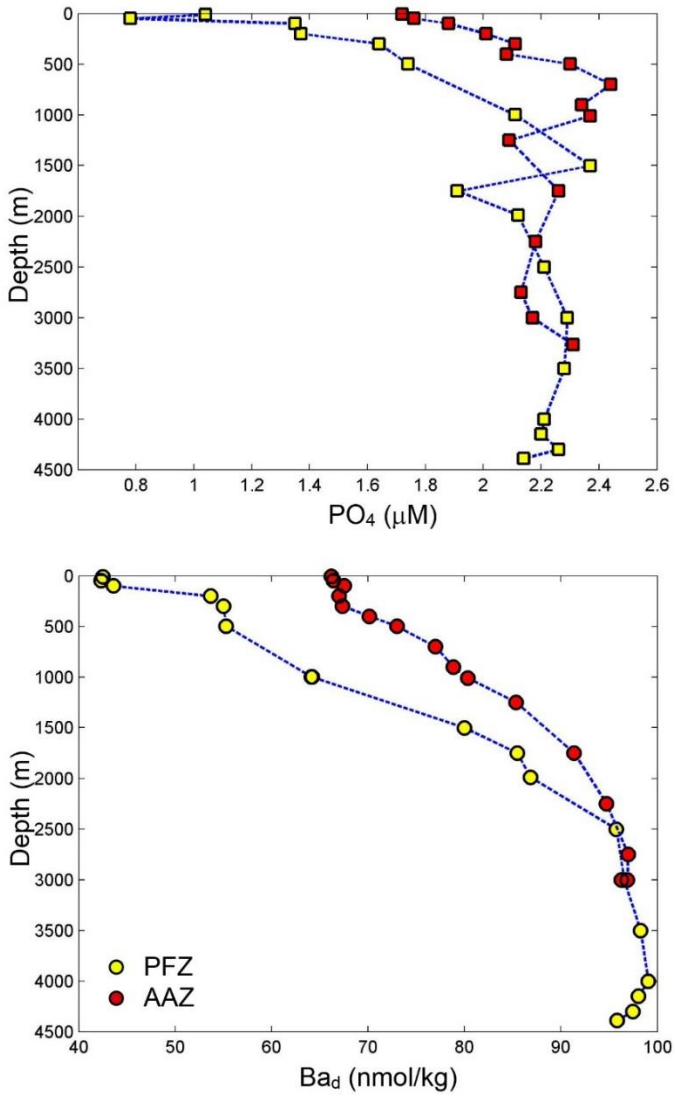

Figure S8: *Depth profiles of phosphate (squares) and dissolved barium (circles) from two stations: Station 33 from the PFZ (yellow) and Station 26 from the AAZ (red). The profiles highlight the difference in remineralisation depths of barium and organic matter.*

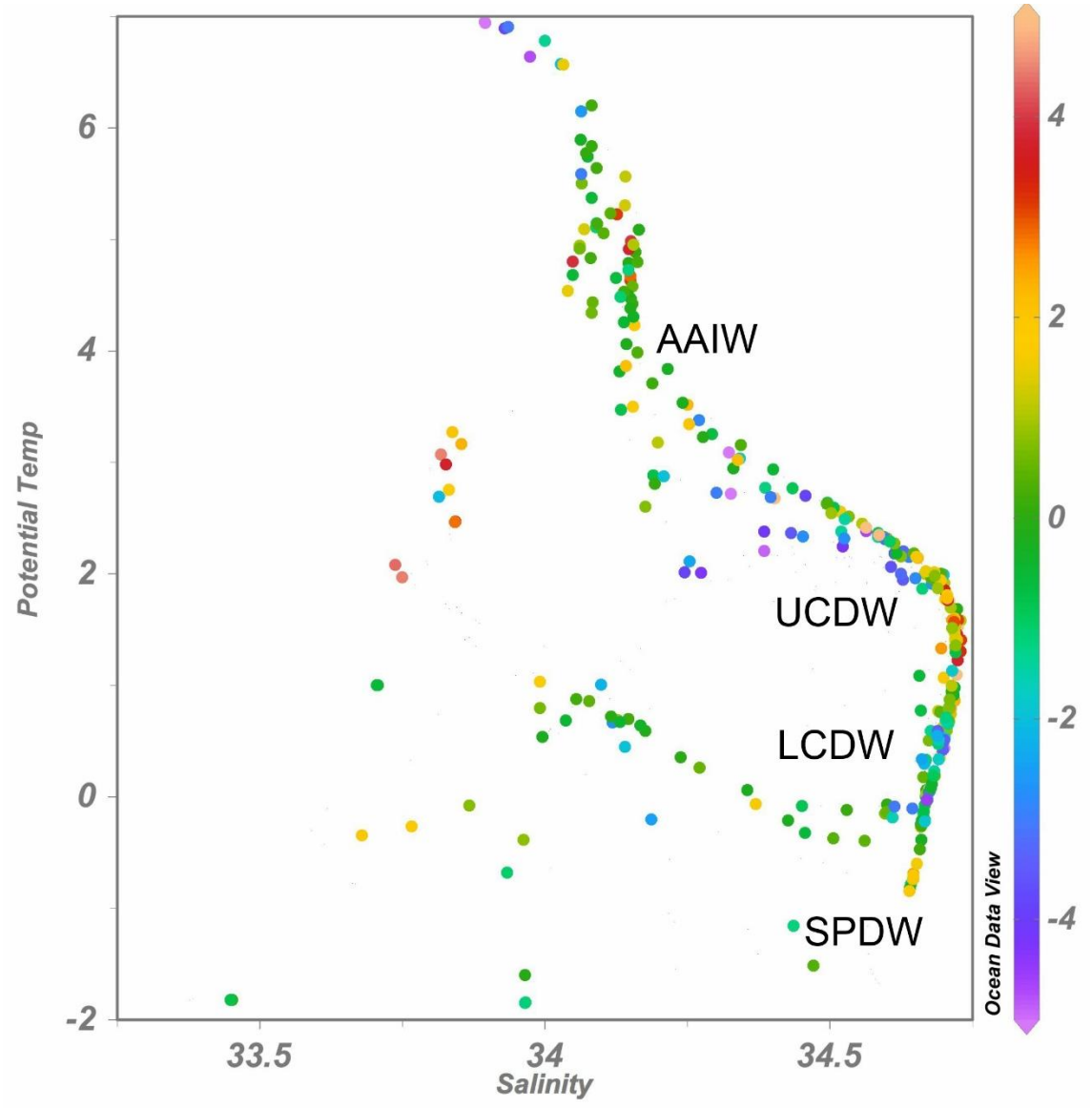

Figure S9: *Potential temperature (°C) and salinity plot, plotted versus* $Ba_d^{Si\ residual}$*. Colour scale represents* $Ba_d^{Si\ residual}$ *(nmol* kg^{-1}*) in the water column. Main water masses labelled: Antarctic Intermediate Water (AAIW), Upper and Lower Circumpolar Deep Waters (UCDW and LCDW), South Pacific Deep Water (SPDW). Note positive residuals within the UCDW water mass (see main text for discussion).*

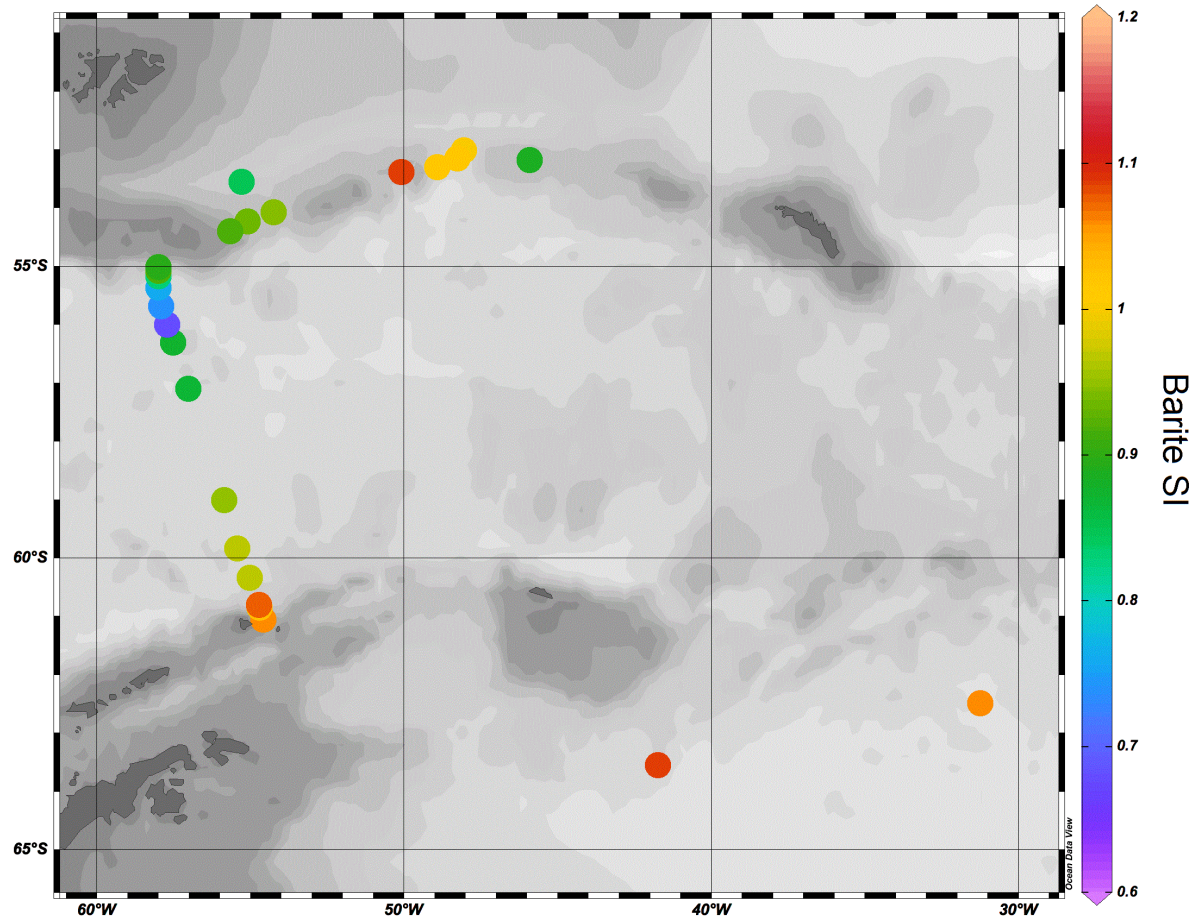

Figure S10: *Estimated surface water barite saturation states (see above for details). Plot made using Ocean Data View version 4.*

References

Bendschneider, K. and Robinson, R.J., 1952. A new spectrophotometric method for the determination of nitrite in sea water.

Graham, R.M., Boer, A.M., Heywood, K.J., Chapman, M.R. and Stevens, D.P., 2012. Southern Ocean fronts: Controlled by wind or topography? Journal of Geophysical Research: Oceans, 117(C8).

Gruber, N., 2008. The marine nitrogen cycle: overview and challenges. Nitrogen in the marine environment, 2: 1-50.

Monnin, C., 1999. A thermodynamic model for the solubility of barite and celestite in electrolyte solutions and seawater to 200 C and to 1 kbar. Chemical Geology, 153(1): 187-209.

Murphy, J. and Riley, J.P., 1962. A modified single solution method for the determination of phosphate in natural waters. Analytica chimica acta, 27: 31-36.

Naveira Garabato, A.C., Heywood, K.J. and Stevens, D.P., 2002. Modification and pathways of Southern Ocean deep waters in the Scotia Sea. Deep-Sea Research I, 49: 681-705.

Orsi, A.H., Whitworth, T. and Nowlin, W.D., 1995. On the meridional extent and fronts of the Antarctic Circumpolar Current. Deep Sea Research Part I: Oceanographic Research Papers, 42(5): 641-673.

Thomas, H. et al., 2011. Barium and carbon fluxes in the Canadian Arctic Archipelago. Journal of Geophysical Research: Oceans, 116(C9).